Dynamics of Ultrafast Intramolecular Charge Transfer with 1-*tert*-Butyl-6-cyano-1,2,3,4-tetrahydroquinoline (NTC6) in *n*-Hexane and Acetonitrile

Sergey I. Druzhinin,*,† Sergey A. Kovalenko,*,‡ Tamara Senyushkina,†,‡ and Klaas A. Zachariasse*,†

Spektroskopie und Photochemische Kinetik, Max-Planck-Institut für biophysikalische Chemie, 37070 Göttingen, Germany, and Institut für Chemie, Humboldt Universität zu Berlin, Brook-Taylor Strasse 2, 12489 Berlin, Germany

Received: June 26, 2007; In Final Form: October 2, 2007

The intramolecular charge transfer (ICT) reaction of 1-*tert*-butyl-6-cyano-1,2,3,4-tetrahydroquinoline (NTC6) in *n*-hexane and acetonitrile (MeCN) is investigated by picosecond fluorescence experiments as a function of temperature and by femtosecond transient absorption measurements at room temperature. NTC6 in *n*-hexane is dual fluorescent from a locally excited (LE) and an ICT state, with a quantum yield ratio Φ'(ICT)/Φ(LE) of 0.35 at +25 °C and 0.67 at −95 °C, whereas in MeCN mainly an ICT emission is observed. From the temperature dependence of Φ'(ICT)/Φ(LE) for NTC6 in *n*-hexane, an LE/ICT enthalpy difference ΔH of −2.4 kJ/mol is determined. For comparison, 1-isopropyl-6-cyano-1,2,3,4-tetrahydroquinoline (NIC6) is also investigated. This molecule does not undergo an ICT reaction, because of its larger energy gap $\Delta E(S_1,S_2)$. From the molar absorption coefficient ϵ^{max} of NTC6 as compared with other aminobenzonitriles, a ground-state amino twist angle θ of ∼22° is deduced. The increase of ϵ^{max} between *n*-hexane and MeCN indicates that θ decreases when the solvent polarity becomes larger. Whereas single-exponential LE fluorescence decays are obtained for NIC6 in *n*-hexane and MeCN, the LE and ICT decays of NTC6 in these solvents are double exponential. For NTC6 in *n*-hexane at −95 °C, with a shortest decay time of 20 ps, the forward ($k_a = 2.5 \times 10^{10}$ s^{-1}) and backward ($k_d = 2.7 \times 10^{10}$ s^{-1}) rate constants for the LE ↔ ICT reaction are determined from the time-resolved LE and ICT fluorescence spectra. For NTC6 in *n*-hexane and MeCN, the excited-state absorption (ESA) spectrum at 200 fs after excitation is similar to the LE(ESA) spectra of NIC6 and 4-(dimethylamino)benzonitrile (DMABN), showing that LE is the initially excited state for NTC6. These results indicate that the LE states of NTC6, NIC6, and DMABN have a comparable molecular structure. The ICT(ESA) spectrum of NTC6 in *n*-hexane and MeCN resembles that of DMABN in MeCN, likewise indicating a similar ICT structure for NTC6 and DMABN. From the decay of the LE absorption and the corresponding growing-in for the ICT state of NTC6, it is concluded that the ICT state originates from the LE precursor and is not formed by direct excitation from S_0, nor via an S_2/ICT conical intersection. The same conclusion was made from the time-resolved (picosecond) fluorescence spectra, where there is no ICT emission at time zero. The decay of the LE(ESA) band of NTC6 in *n*-hexane occurs with a shortest time τ_2 of 2.2 ps. The ICT reaction is much faster ($\tau_2 = 0.82$ ps) in the strongly polar MeCN. The absence of excitation wavelength dependence (290 and 266 nm) for the ESA spectra in MeCN also shows that LE is the ICT precursor. With NIC6 in *n*-hexane and MeCN, a decay or growing-in of the femtosecond ESA spectra is not observed, in line with the absence of an ICT reaction involving an S_2/ICT conical intersection.

Introduction

Rigidized aminobenzonitriles such as 1-methyl-6-cyano-1,2,3,4-tetrahydroquinoline (NMC6),[1,2] 1-ethyl-6-cyano-1,2,3,4-tetrahydroquinoline (NEC6),[3] and 1-isopropyl-6-cyano-1,2,3,4-tetrahydroquinoline (NIC6)[3] have played an important role in the investigation of the intramolecular charge transfer (ICT) taking place with electron donor(D)/acceptor(A) benzenes, among which 4-(dimethylamino)benzonitrile (DMABN) is the central representative. The absence of ICT and dual fluorescence with NMC6[1−3] and, in particular, with the planarized molecules 1-methyl-5-cyanoindoline (NMC5),[2,4,5] 1-ethyl-5-cyanoindoline (NEC5),[3,6] and 1-ispropyl-5-cyanoindoline (NIC5),[3] has been seen[4−7] as the most important experimental support for the twisted intramolecular charge transfer (TICT) model. With 1-*tert*-butyl-6-cyano-1,2,3,4-tetrahydroquinoline (NTC6), however, fast and efficient ICT has been observed in a large series of solvents, from the nonpolar alkanes to the polar acetonitrile and methanol.[3] The dipole moment μ_e(ICT) of the ICT state of NTC6 (19 D), determined from its solvatochromic shift relative to that of DMABN or 4-(diisopropylamino)benzonitrile (DIABN), was found to be larger than that of DMABN (17 D) and DIABN (17 D).[3] For the locally excited (LE) state of NMC6 and NIC6 a considerably smaller dipole moment μ_e(LE) of around 11 D was determined. The μ_e(LE) of NTC6 could not be obtained directly from a solvatochromic plot as the fluorescence bands of the LE and ICT states of NTC6 strongly overlap.[3] It was concluded from NTC6[3] and likewise from fluorazene,[8]

* Corresponding authors. E-mails: S.I.D., sdruzhi@gwdg.de; S.A.K., skovale@chemie.hu-berlin.de; K.A.Z., kzachar@gwdg.de. Fax: +49-551-201-1501.

† Max-Planck-Institut für biophysikalische Chemie.

‡ Humboldt Universität zu Berlin.

10.1021/jp074983z CCC: $37.00 © 2007 American Chemical Society
Published on Web 11/23/2007

CHART 1

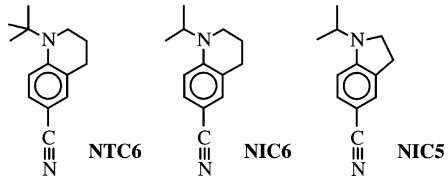

that for ICT with aminobenzonitriles and related molecules a full 90° amino twist (TICT) and hence a complete electronic decoupling of the amino (D) and benzonitrile (A) moieties is not required. It has further been assumed that the ICT state cannot be populated by direct absorption from S_0 but is formed from the equilibrated lowest excited singlet state S_1(LE) as the precursor.[2,3]

Recently, theoretical studies on the energies of the LE and ICT states of NTC6 and NMC6 have appeared.[9−11] These three calculations all attribute the appearance of ICT emission with NTC6 in *n*-hexane and its absence with NMC6 and DMABN in this solvent to the relatively small energy gap $\Delta E(S_1,S_2)$ between the two lowest excited singlet states of the former molecule. This finding supports our conclusion on the essential importance of $\Delta E(S_1,S_2)$ for ICT in aminobenzonitriles.[3,8] Different from our opinion,[3] however, it is found in refs 10 and 11 that the molecular structure of the ICT state of NTC6 has a substantially twisted amino group, with a computed twist angle θ of 69 or 65°, as compared with 35 or 39° for LE and 35 or 28° for S_0. This ICT state was therefore termed TICT, in contrast to a planar intramolecular charge transfer (PICT)[3,8] state. It is of interest to note that in refs 10 and 11 the suggestion is made that the ICT state of NTC6, as well as that of DMABN, can be populated by direct absorption from the ground state to a Franck−Condon S_2 state, via a conical intersection of the S_2 and ICT potential energy surfaces.

In discussing the TICT/PICT issue, it is important to recall that TICT stands for a full (perpendicular) amino twist and a complete electronic decoupling of the D and A subgroups. The opposite PICT concept would possibly not have been introduced[12] when TICT would have been less demanding. It certainly does not intend to claim that the ICT amino twist angle should be zero degrees. Therefore, adapting TICT to make it also applicable to smaller twist angles than perpendicular, for which the D/A-electronic coupling may be substantial, is not in line with the original concept.[13] It is hence advisable to emphasize the extent of electronic D/A coupling in an ICT state, rather than the extremes of the amino twist angle.

In the present paper, absorption and fluorescence spectra of NTC6 and NIC6 in *n*-hexane and MeCN as a function of temperature are reported. From the analysis of the LE and ICT fluorescence quantum yields in *n*-hexane, the ΔH of the ICT reaction is determined. Molar absorption coefficients are measured to determine the amino twist angle in solution. Picosecond fluorescence decays of NTC6 in *n*-hexane and MeCN at several temperatures are discussed, together with femtosecond transient absorption spectra of NTC6 at room temperature in these solvents. Similar experiments are carried out with NIC6,[3] a NTC6 derivative for which an ICT reaction does not take place.

Experimental Section

The synthesis of NTC6 (mp 130.8−131.0 °C) and NIC6 has been described previously.[3] HPLC was the last purification step. The solvent *n*-hexane (Merck, Uvasol) was used as received, whereas acetonitrile (MeCN, Merck, Uvasol) was chromatographed over Al_2O_3. The solutions, with an optical density between 0.4 and 0.6 at the maximum of the first band in the absorption spectrum, were deaerated by bubbling with nitrogen for 15 min. The measurement of the absorption and fluorescence spectra and the fluorescence quantum yields was described earlier.[14] The fluorescence quantum yield Φ_f was corrected for the temperature dependence of the optical density of the solution by measuring the absorption spectrum of NTC6 and NIC6 as a function of temperature. In the determination of the temperature dependence of Φ_f, the change in optical density with temperature and its nonlinear effect on the fluorescence intensity were

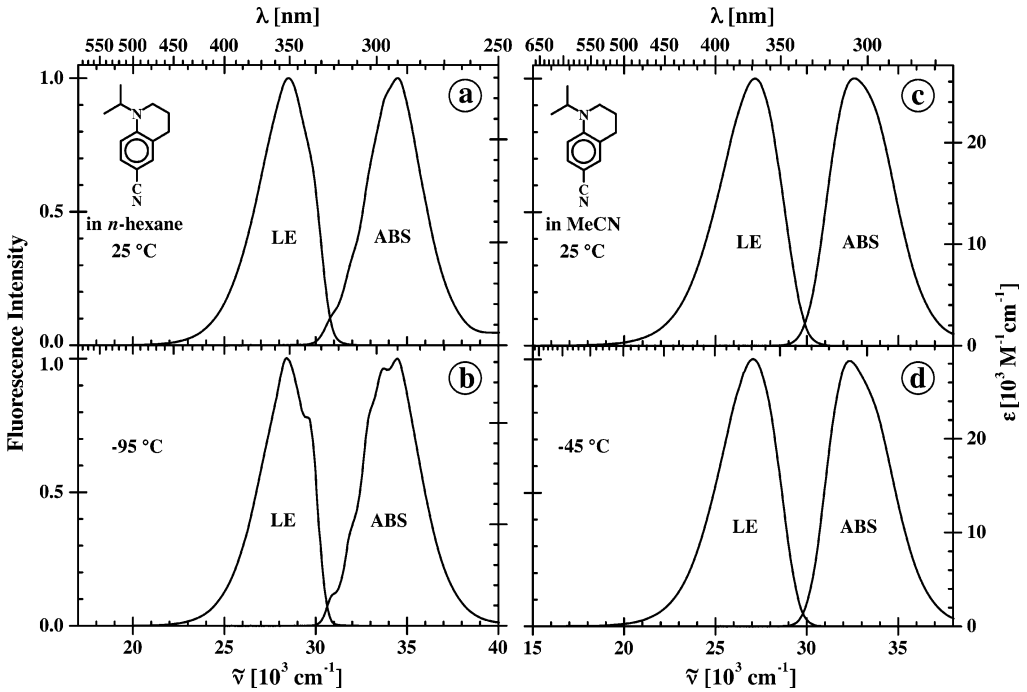

Figure 1. Absorption and LE fluorescence spectra of 1-isopropyl-6-cyano-1,2,3,4-tetrahydroquinoline (NIC6) in *n*-hexane at (a) +25 °C and (b) −95 °C and in acetonitrile (MeCN) at (c) +25 and (d) −45 °C.

TABLE 1: Data Obtained from the Fluorescence and Absorption Spectra of NIC6 and NTC6 in *n*-Hexane and Acetonitrile (MeCN)

solvent	NIC6				NTC6			
	n-hexane		MeCN		*n*-hexane		MeCN	
T (°C)	−95	25	−45	25	−95	25	−45	25
Φ(LE)	0.225	0.194	0.250	0.245	0.228	0.159	*a*	*a*
Φ'(ICT)	0	0	0	0	0.153	0.056	0.564	0.597
Φ'(ICT)/Φ(LE)	0	0	0	0	0.67	0.35		
Φ(ISC)[b]						0.31		0.31[c]
$\tilde{\nu}^{max}$ (total,fl) [cm^{-1}]	28450	28510	27050	27130	27870	28170	22600	23130
$\tilde{\nu}^{max}$ (abs) [cm^{-1}]	34430	34460	32360	32600	32890	33390	31910	32100
ϵ^{max} [M^{-1} cm^{-1}]	26320	25930	28270	26290	25820	22040	28460	25780
$E(S_1)^{fl}$ [cm^{-1}][d]	30640	30790	29790	29890	30790	30860	28790	28880
σ(abs) [10^{-17} cm^2][e]	4.37	4.31	4.69	4.37	4.29	3.66	4.73	4.28
σ(em) [10^{-17} cm^2][f]	1.64	1.51	2.24	2.21			1.49	1.52
$E(S_1)^{cs}$ [cm^{-1}][g]	30620	30760	29750	29840	30760	30820	28650	28760

[a] Total fluorescence spectrum consists mainly of ICT emission. The precise contribution of the LE emission cannot be established. [b] Measurements as in ref 21. [c] The triplet yield of NTC6 in MeCN is reproduced, using 308 nm excitation and perylene (ref 21). [d] Crossing point of the fluorescence and absorption spectra (Figures 2 and 5). [e] Absorption cross section σ(abs) (Figure S1 in Supporting Information). [f] Emission cross section σ(em) (Figure S1). [g] Crossing point of the emission and absorption cross section spectra (Figure S1).

accounted for by using absorption spectra measured over the relevant temperature range.

The fluorescence decay times were obtained with a picosecond laser (λ_{exc}: 276 nm) single-photon counting (SPC) system,[15,16] two time ranges being routinely measured simultaneously (0.5 and 10 ps/channel in up to 1800 effective channels). The estimated reproducibility is better than 10% for the picosecond decay times. The time-resolved fluorescence spectra of NTC6 in *n*-hexane at −95 °C were separated into their LE and ICT contributions by varying the amplitudes and spectral shifts for the LE and ICT steady-state fluorescence spectra measured at the same temperature. The femtosecond transient absorption setup has been described in detail elsewhere.[17,18] NTC6 and NIC6 in *n*-hexane or acetonitrile at room temperature (22 °C) were excited with 1 μJ, 70 fs pulses at 290 or 266 nm. The pump-induced transient absorption signal was monitored with a supercontinuum probe in the range 334−1072 nm.[14]

Results and Discussion

Absorption and Fluorescence Spectra of NIC6. *In n-Hexane at +25 and −95 °C.* The absorption and fluorescence spectra of NIC6 in *n*-hexane at +25 and −95 °C are shown in Figure 1a,b. The absorption spectrum at 25 °C (Figure 1a) consists of a main band attributed to S_2, with a maximum $\tilde{\nu}^{max}$(abs) at 34460 cm^{-1}, and a much weaker structured band on the leading edge of the absorption spectrum (at 30840 cm^{-1}, shoulder), which corresponds to the $S_0 \rightarrow S_1$ transition.[3] At −95 °C, the structure of the $S_0 \rightarrow S_1$ absorption is more pronounced, with a lowest-energy maximum at around 30930 cm^{-1}. The fluorescence spectrum of NIC6 in *n*-hexane consists of a single LE emission with some vibrational structure, at +25 as well as at −95 °C, with $\tilde{\nu}^{max}$(abs) at 28510 and 28450 cm^{-1} (Table 1).

In Acetonitrile at +25 and −45 °C. In the absorption spectrum of NIC6 in MeCN at +25 and −45 °C with maxima at 32600 and 32360 cm^{-1} (Figure 1c,d), the structured S_1 absorption is no longer visible. It is covered by the broad band of S_2, due to the larger spectral shift (1860 cm^{-1} at 25 °C) of the latter as compared with that of S_1 in this solvent, caused by its stronger polar character.[3,7−11,19] The fluorescence spectrum of NIC6 in the polar solvent MeCN remains a single LE band at both temperatures, i.e., intramolecular charge transfer (ICT) does not take place with NIC6 in MeCN at +25 and −45 °C.[3]

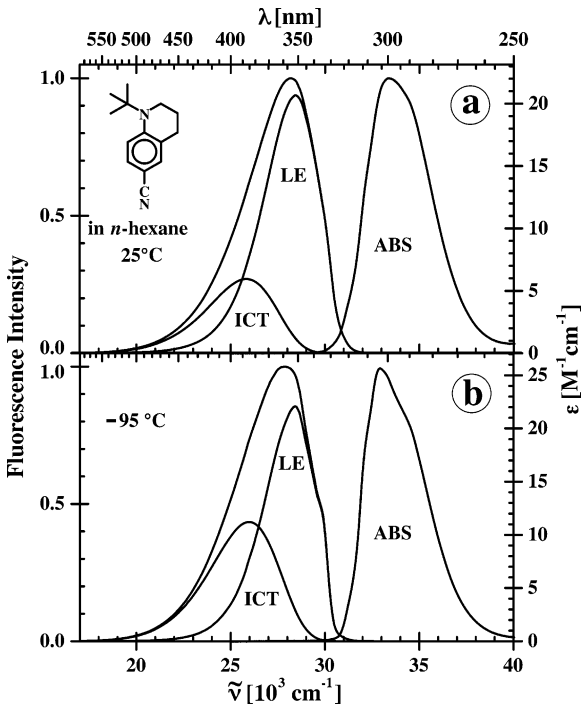

Figure 2. Absorption and fluorescence spectra of 1-*tert*-butyl-6-cyano-1,2,3,4-tetrahydroquinoline (NTC6) in *n*-hexane at (a) +25 °C and (b) −95 °C. The overall fluorescence spectra are separated into the contributions of the LE and ICT emissions; see text.

Absorption and Fluorescence Spectra of NTC6. *In n-Hexane at +25 and −95 °C.* The absorption spectra of NTC6 in *n*-hexane at +25 and −95 °C in Figure 2 consist of a broad band ($\tilde{\nu}^{max}$(abs) at 33390 and 32890 cm^{-1}), without an indication of a structured S_1 absorption at its red edge, showing that the energy gap $\Delta E(S_1,S_2)$ of NTC6 is smaller than that of NIC6; see Figure 1. At both temperatures, dual fluorescence is observed. The separation of the total fluorescence spectra into their LE and ICT components was carried out by making the assumption that for NTC6 the shape of the LE emission band is similar to that of NIC6, whereas the ICT emission band of NTC6 is taken to be equal to that of DIABN, in both cases measured in *n*-hexane at the same temperature.[20] The ICT-to-LE-fluorescence quantum yield ratio Φ'(ICT)/Φ(LE) increases from 0.35 at +25 °C to 0.67 at −95 °C, indicating that $-\Delta H$

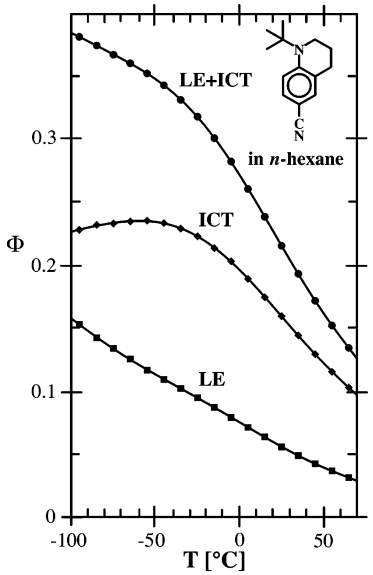

Figure 3. Plots of the total fluorescence quantum yield Φ(LE +ICT) and the separate quantum yields Φ′(ICT) and Φ(LE) of 1-*tert*-butyl-6-cyano-1,2,3,4-tetrahydroquinoline (NTC6) in *n*-hexane as a function of temperature.

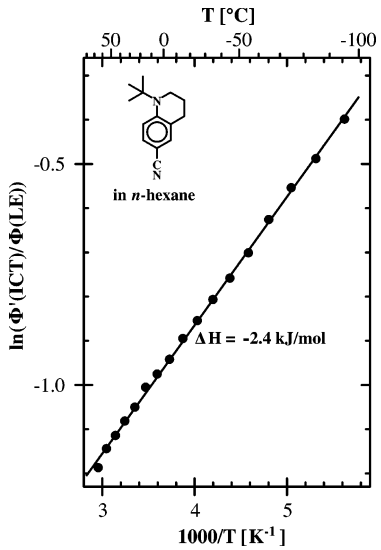

Figure 4. Plot of ln(Φ′(ICT)/Φ(LE)) *versus* the reciprocal absolute temperature for 1-*tert*-butyl-6-cyano-1,2,3,4-tetrahydroquinoline (NTC6) in *n*-hexane over the temperature range from +65 to −95 °C. The slope of the plot, equal to $-\Delta H/R$ (eq 2), results in a value of −2.4 kJ/mol for the LE → ICT enthalpy difference Δ*H*; see text.

for the ICT reaction with NTC6 in *n*-hexane is relatively small (see below).

LE and ICT Fluorescence Quantum Yields of NTC6 in *n*-Hexane as a Function of Temperature. The total fluorescence quantum yield of NTC6 in *n*-hexane was measured as a function of temperature from +65 to −95 °C. From the overall fluorescence spectra, the fluorescence quantum yields Φ′(ICT) and Φ(LE) were determined (see Figure 3). It is seen that Φ(LE) increases upon cooling, from 0.03 at 65 °C to 0.16 at −95 °C, whereas Φ′(ICT) changes from 0.10 to 0.23, with a maximum of 0.24 at around −60 °C.

ICT Enthalpy Difference ΔH of NTC6 in *n*-Hexane. The plot of the natural logarithm of the quantum yield ratio Φ′(ICT)/Φ(LE) versus 1000/*T* for NTC6 in *n*-hexane (Figure 4) shows a linear increase, which means that the system is in the high-temperature limit (HTL) over the entire temperature

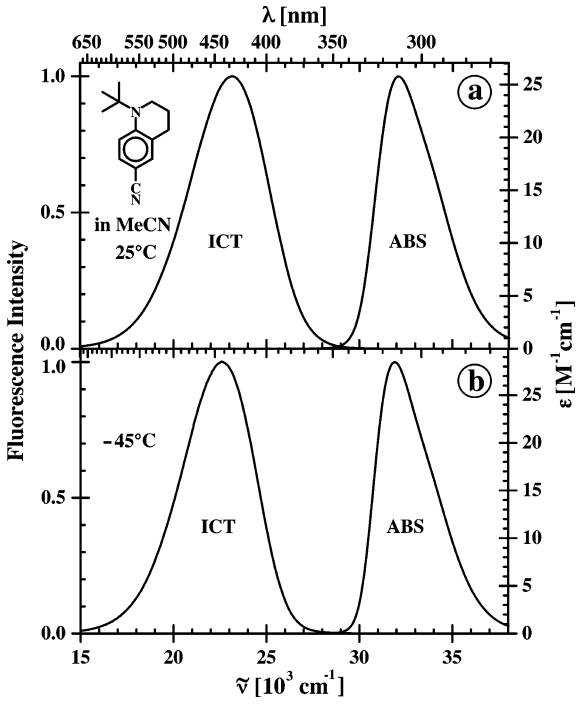

Figure 5. Absorption and fluorescence spectra of 1-*tert*-butyl-6-cyano-1,2,3,4-tetrahydroquinoline (NTC6) in acetonitrile (MeCN) at (a) +25 °C and (b) −45 °C. The fluorescence spectrum consists of an ICT emission, without clear evidence for an LE fluorescence. In the absorption spectra the S_1 band is not visible; see text and Figure 1.

SCHEME 1

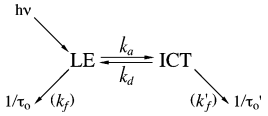

range between 65 and −95 °C, with the condition $k_d \gg 1/\tau'_0$(ICT); see eqs 1 and 2.[2,14] Under these HTL conditions, the slope of the plot is equal to $-\Delta H/R$, where Δ*H* is the enthalpy difference for the equilibrated LE → ICT reaction and *R* is the gas constant, giving a value of −2.4 kJ/mol for Δ*H*.

$$\frac{\Phi'(\mathrm{ICT})}{\Phi(\mathrm{LE})} = \frac{k'_\mathrm{f}(\mathrm{ICT})}{k_\mathrm{f}(\mathrm{LE})}\,\frac{k_\mathrm{a}}{k_\mathrm{d} + 1/\tau'_0(\mathrm{ICT})} \qquad (1)$$

Under HTL-conditions ($k_d \gg 1/\tau'_0$(ICT)), eq 1 simplifies to

$$\frac{\Phi'(\mathrm{ICT})}{\Phi(\mathrm{LE})} = \frac{k'_\mathrm{f}(\mathrm{ICT})}{k_\mathrm{f}(\mathrm{LE})}\,\frac{k_\mathrm{a}}{k_\mathrm{d}} \qquad (2)$$

In eqs 1 and 2 and Scheme 1, k_a and k_d are the rate constants of the forward and backward ICT reaction, τ_0(LE) and τ'_0(ICT) are the fluorescence lifetimes, whereas k_f(LE) and k'_f(ICT) are the radiative rate constants.

In Acetonitrile at +25 and −45 °C. The maximum of the broad absorption spectra of NTC6 in MeCN (Figure 5) undergoes a red shift upon cooling, from 32100 cm^{-1} at +25 °C to 31910 cm^{-1} at −45 °C (Table 1), in accordance with the identification of this band as an $S_0 \rightarrow S_2$ transition.[3] In the absorption spectrum, the S_1 transition is not visible due to the overlapping S_2 absorption, similar to what was observed with NIC6 (Figure 1).

The fluorescence spectrum of NTC6 in MeCN at +25 and −45 °C (Figure 5) consists of an ICT emission band, without clear evidence for an LE fluorescence. Note, however, the empty

TABLE 2: Decadic Molar Absorption Coefficients, ϵ^{max}, Measured at the Maximum, λ^{max}, of the Main Lowest-Energy Absorption Band of Compounds NXC6, DMABN, and NXC5 in *n*-Hexane and Acetonitrile (MeCN) at 25 °C (Figures 1, 2, and 5)

solvent (dielectric constant)		NTC6	NIC6	NEC6	NMC6	DMABN	NIC5	NEC5	NMC5
n-hexane (1.88)	ϵ^{max} [M^{-1} cm^{-1}]	22085[a]	26220[b]	26005	25410	29370	23465	22000	21445
	λ^{max} [nm]	299.7	290.0	289.3	287.5	280.7	291.0	289.7	287.6
MeCN (36.7)	ϵ^{max} [M^{-1} cm^{-1}]	25800[c]	26540[d]	25850	24980	27755[e]			
	λ^{max} [nm]	311.8	306.9	306.2	304.0	292.1			

[a] 3080 M^{-1} cm^{-1} at 266 nm. [b] 20110 M^{-1} cm^{-1} at 290 nm. [c] 1370 M^{-1} cm^{-1} at 266 nm. [d] 13520 M^{-1} cm^{-1} at 290 nm. [e] See ref 14, where for DMABN in MeCN $\epsilon^{max} = 27990$ M^{-1} cm^{-1} at 292.0 nm.

TABLE 3: Decadic Molar Absorption Coefficients, ϵ^{max}, Measured at the Maximum, λ^{max}, of the Lowest-Energy Absorption Band of NTC6 in Various Solvents at 25 °C

solvent	*n*-hexane	DBE[a]	DEE[b]	THF[c]	MeCN
$\epsilon^{d,e}$	1.88	3.05	4.24	7.39	36.7
ϵ^{max} [M^{-1} cm^{-1}]	22085	22755	23585	24980	25800
λ^{max} [nm]	299.7	303.6	303.9	308.3	311.8

[a] Di-*n*-butyl ether. [b] Diethyl ether. [c] Tetrahydrofuran. [d] Dielectric constant at 25 °C. [e] Reference 26.

spectral space between the absorption and emission spectra at −45 °C, which is indicative of a short-lived LE emission, as will be substantiated in a later section. The ICT emission maximum $\tilde{\nu}^{max}$(ICT) shifts to the red from 23130 cm^{-1} at +25 °C to 22600 cm^{-1} at −45 °C, due to its large dipole moment of 19 D and the increase of the solvent polarity upon cooling.[14,19]

Molar Absorption Coefficients and Amino Twist Angle of NXC6 and NXC5 in S_0. The decadic molar absorption coefficient ϵ^{max} of the maximum of the lowest-energy absorption band of NTC6 in *n*-hexane at 25 °C (Figure 2a) is with 22085 M^{-1} cm^{-1} considerably lower than that of the three other 1-alkyl-6-cyano-1,2,3,4-tetrahydroquinolines NIC6, NEC6, and NMC6 in this solvent, for which ϵ^{max} ranges between 26220 and 25410 M^{-1} cm^{-1} (Table 2).[22] On the basis of the observation that for 4-aminobenzonitriles the amino twist angle θ in the ground state S_0 determines ϵ^{max} according to the relation $\epsilon^{max} \sim \cos^2 \theta$,[23,24] an amino twist angle of 22.8° (NEC6) or 21.2° (NMC6) is derived for NTC6 in *n*-hexane, depending on which molecule (NEC6 or NMC6) is taken to have a nontwisted amino nitrogen. This result is in good agreement with the amino twist angle $\theta = 22.7°$ obtained from the X-ray structure analysis for NTC6, to be discussed separately.[25]

Influence of Solvent Polarity on Molar Absorption Coefficient of NTC6. In MeCN, somewhat surprisingly, the difference between the ϵ^{max} of NTC6 and that of NIC6, NEC6, and NMC6 is much smaller than in *n*-hexane (Table 3). From the ϵ^{max} of NTC6 (25800 M^{-1} cm^{-1}) and NIC6 (26540 M^{-1} cm^{-1}) in MeCN, an approximate twist angle θ of 9.6° is calculated for NTC6, via $\epsilon^{max} \sim \cos^2 \theta$ and an assumed planar amino group in NIC6; see previous section. When the solvent polarity becomes larger, such as in the series *n*-hexane, di-*n*-butyl ether, diethyl ether, tetrahydrofuran, MeCN (Table 3), ϵ^{max} of NTC6 gradually increases. This result could indicate that the amino twist angle of NTC6 is affected by interaction with the solvent, the molecule becoming more planar with increasing solvent polarity.

Single-Exponential Picosecond Fluorescence Decays of NIC6 in *n*-Hexane and Acetonitrile. The fluorescence decays i_f of NIC6 are single exponential over the entire temperature ranges investigated (time resolution 2 ps/channel), from +65 to −95 °C in *n*-hexane and from +75 to −45 °C in MeCN. The single-exponential character of these LE decays, also at low temperatures (Figure 6) where conditions are usually optimal for marginal systems with a small $-\Delta H$ for the LE → ICT reaction,[2,14,27] supports the absence of ICT fluorescence in the emission spectra of NIC6 shown in Figure 1. The fluorescence lifetime τ_0(LE) of NIC6 in *n*-hexane ranges from 2.8 ns at +65 °C to 3.1 ns at to −95 °C and in MeCN from 2.6 ns at +75 °C to 2.7 ns at to −45 °C; see Figure 7 in the following section.

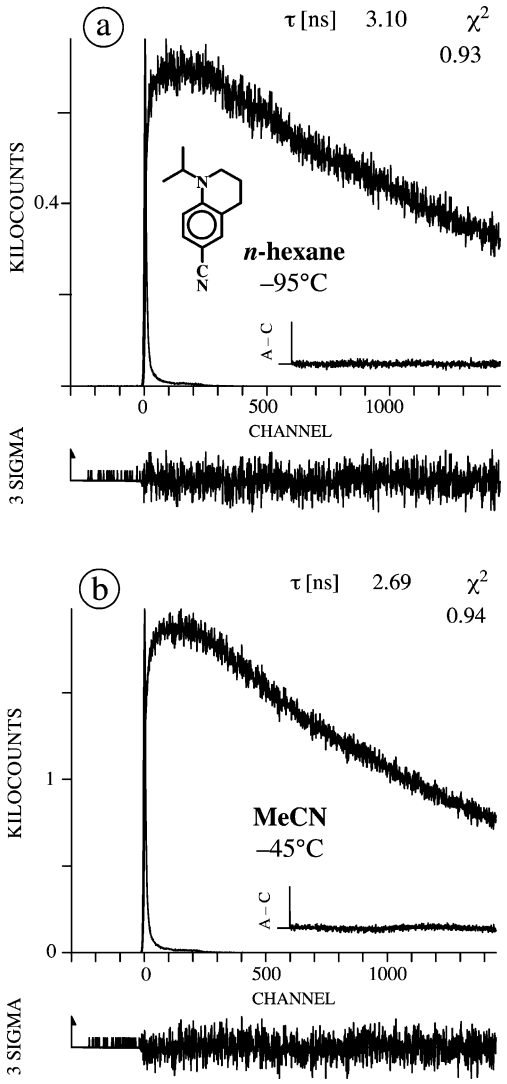

Figure 6. Single-exponential LE fluorescence decays of 1-isopropyl-6-cyano-1,2,3,4-tetrahydroquinoline (NIC6) (a) in *n*-hexane at −95 °C and (b) in acetonitrile (MeCN) at −45 °C. The emission wavelengths are (a) 330 nm and (b) 370 nm. The decay time τ and the values for χ^2 are given in the figure. The weighted deviations σ and the autocorrelation functions A−C are also indicated. Excitation wavelength λ_{exc}: 276 nm. Time resolution: 2.0 ps/channel with a time window of 1500 effective channels.

LE Fluorescence Quantum Yield and Lifetime of NIC6 in *n*-Hexane and Acetonitrile as a Function of Temperature. The temperature dependence of the fluorescence quantum yield Φ(LE) of NIC6 in *n*-hexane and MeCN is plotted in Figure 7b.

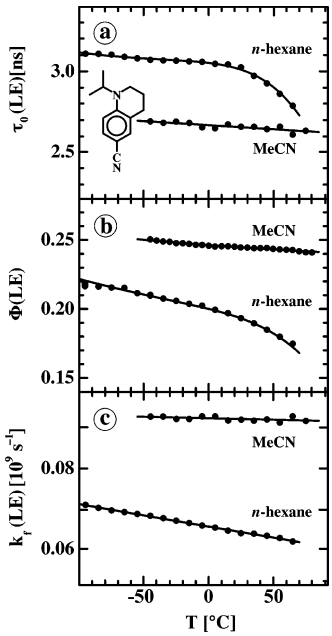

Figure 7. Temperature dependence of (a) the fluorescence decay time τ_0(LE), (b) the LE fluorescence quantum yield Φ(LE) and (c) the radiative rate of k_f for 1-isopropyl-6-cyano-1,2,3,4-tetrahydroquinoline (NIC6) in *n*-hexane and acetonitrile (MeCN).

From Φ(LE) and the corresponding fluorescence decay times τ_0(LE) in Figure 7a, the radiative rate constants k_f(LE) of NIC6 in *n*-hexane and MeCN are calculated by using the relation $k_f(\mathrm{LE}) = \Phi(\mathrm{LE})/\tau_0(\mathrm{LE})$ (see Figure 7c), to be able to compare these k_f(LE) data with those of NTC6 in MeCN in a following section. For NIC6 in *n*-hexane, the radiative rate constant k_f(LE) becomes somewhat smaller with increasing temperature, from 7.1×10^7 s^{-1} at -95 °C to 6.2×10^7 s^{-1} at $+65$ °C, similar to what has been observed[14] previously for DMABN in *n*-hexane and MeCN. This has been explained via the relationship $k_f = k_f(0)n^2$, where n is the solvent refractive index and $k_f(0)$ is temperature independent.[28] The refractive index n in *n*-hexane becomes smaller with increasing temperature.[29] For NIC6 in MeCN, however, k_f(LE) remains practically constant, increasing between -45 and $+75$ °C from 9.2×10^7 to 9.3×10^7 s^{-1}.

Picosecond LE and ICT Fluorescence Decays of NTC6 in *n*-Hexane and Acetonitrile. ***NTC6 in n-Hexane.*** The LE and ICT fluorescence decays i_f(LE) and i_f(ICT) of NTC6 in *n*-hexane (Figure 8) are double exponential (eqs 3 and 4), at $+25$ °C as well as at -95 °C. Between these temperatures, the shortest apparent decay time τ_2 increases from 2.1 to 20 ps, τ_1 becomes somewhat longer (from 2.44 to 3.99 ns) and the LE amplitude ratio A (eq 5) increases from 0.43 to 1.08. At both temperatures, the ICT amplitudes (eq 4) are equal and of opposite sign ($A_{22} + A_{21} = 0$). This indicates that the ICT concentration [ICT] = 0 at time zero, which means that the ICT state is exclusively formed from the initially excited equilibrated LE state.[2,14] In other words, there is no experimental evidence for a reaction $S_2 \rightarrow$ ICT, nor for direct population of the ICT state by absorption from the S_0 ground state.[2,3,14,30]

$$i_f(\mathrm{LE}) = A_{11}\exp(-t/\tau_1) + A_{12}\exp(-t/\tau_2) \quad (3)$$

$$i_f(\mathrm{ICT}) = A_{21}\exp(-t/\tau_1) + A_{22}\exp(-t/\tau_2) \quad (4)$$

$$A = A_{12}/A_{11} \quad (5)$$

The expressions for τ_1, τ_2, and A appearing in eqs 3−5 are[2,14,31]

$$1/\tau_{1,2} = \frac{1}{2}\{(X+Y) \mp \sqrt{(X-Y)^2 + 4k_a k_d}\} \quad (6)$$

$$A = \frac{X - 1/\tau_1}{1/\tau_2 - X} = \frac{k_a k_d \tau_0^{\,2}}{(1 + k_a\tau_0 - \tau_0/\tau_1)^2} \quad (7)$$

where τ_0 is the fluorescence lifetime of the model compound (no ICT) and X and Y are given by

$$X = k_a + 1/\tau_0 \quad (8)$$

$$Y = k_d + 1/\tau_0' \quad (9)$$

NTC6 in MeCN. The LE and ICT fluorescence decays of NTC6 in MeCN (Figure 9) are double exponential at $+25$ and -45 °C. The shortest times τ_2, 1.8 ps at $+25$ °C and 2.0 ps at -45 °C, are clearly at or beyond the limit of the time-resolution[14] of our SPC measurements. The long decay times τ_1, 10.37 ns (25 °C) and 10.68 ns (-45 °C), are equal to the ICT lifetimes τ_0'(ICT).[2,14,15] Although the time τ_2 obtained from the SPC decay at 25 °C in Figure 9a is longer than the correct time determined from femtosecond transient absorption measurements (0.82 ps, see below), the large amplitude ratios A, 160 at $+25$ °C (a) and 590 at -45 °C (b), indicate[14] that for NTC6 in MeCN the thermal back reaction rate constant k_d is much smaller than the forward LE $\rightarrow$ ICT reaction k_a rate constant (Scheme 1, $A = k_a/k_d$ when $k_d \gg 1/\tau_0'$(ICT))[2,14,15] and becomes smaller upon lowering the temperature.

Fluorescence Quantum Yield Φ'(ICT) and Lifetime τ_0'(ICT) of NTC6 in Acetonitrile as a Function of Temperature. The temperature dependence of the fluorescence decay time τ_1, the fluorescence quantum yield, and the radiative rate constant for NTC6 in MeCN is shown in Figure 10. As there is no evidence for an LE emission in the fluorescence spectra of NTC6 in MeCN (Figure 5), the total fluorescence spectrum is that of the ICT state. Hence, the overall fluorescence quantum yield Φ equals Φ'(ICT), increasing from 0.56 to 0.61 between -45 and $+75$ °C; see Figure 10b. Similarly, the fluorescence decay time τ_1 is equal to the ICT lifetime τ_0'(ICT), decreasing from 10.7 to 9.9 ns between -45 and $+75$ °C (Figure 10a).

From Φ'(ICT) and τ_0'(ICT), the ICT radiative rate constant k_f'(ICT) can be calculated by using the relation $k_f'(\mathrm{ICT}) = \Phi'(\mathrm{ICT})/\tau_0'(\mathrm{ICT})$.[15] The rate constant k_f'(ICT) of NTC6 in MeCN becomes larger with increasing temperature, from 5.3×10^7 to 6.2×10^7 s^{-1} between -45 and $+75$ °C (Figure 10c), in contrast to the decrease of k_f(LE) for NIC6 over this temperature range in MeCN (Figure 7). The temperature dependence of k_f'(ICT) for NTC6 in MeCN observed here is similar to that found for DMABN in this solvent.[14] This indicates that the structure of the ICT state changes with temperature, whereas that of the LE state remains unchanged. It also could reflect the decrease of the energy of the ICT state with increasing solvent polarity upon cooling,[2,14,15,26] which affects the Einstein coefficient (k_f'(ICT)) and hence the transition dipole moment.[31]

Time-Resolved LE and ICT Emission Spectra of NTC6 in *n*-Hexane from SPC Decays at -95 °C. By measuring fluorescence decays over the entire fluorescence band (17 emission wavelengths), the time-resolved LE and ICT emission spectra of NTC6 in *n*-hexane at -95 °C were obtained; see Figure 11. At this temperature, the ICT reaction is with $\tau_2 =$ 20 ps (Figure 8b), well within the experimental time resolution

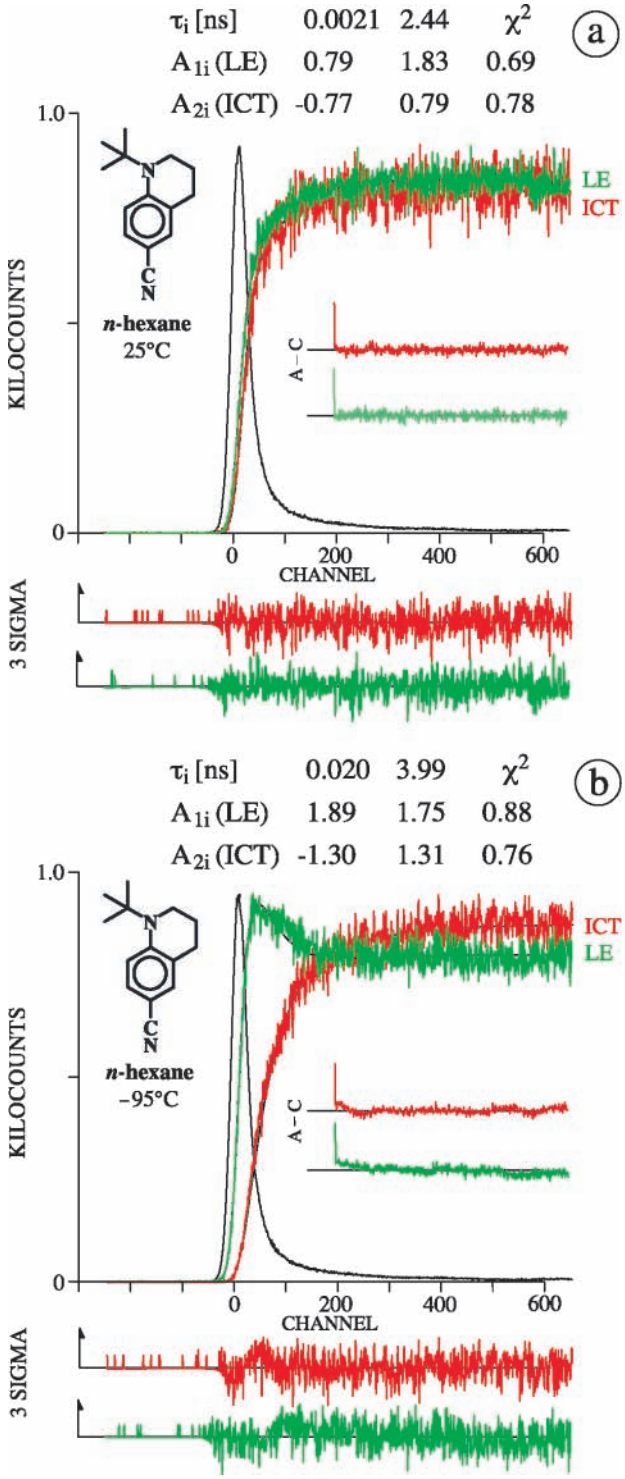

Figure 8. Double exponential LE (340 nm) and ICT (440 nm) fluorescence decays of 1-*tert*-butyl-6-cyano-1,2,3,4-tetrahydroquinoline (NTC6) in *n*-hexane at (a) +25 °C and (b) −95 °C. The decay times τ_2 and τ_1 with the corresponding amplitudes A_{1i}(LE) and A_{2i}(ICT) (see eqs 3−5) are given in the figure. The shortest decay time is listed first. The values for χ^2, the weighted deviations σ and the autocorrelation functions A−C are also indicated. Excitation wavelength λ_{exc}: 276 nm. Time resolution: 0.5 ps/channel with a time window of 650 channels.

of around 3 ps.[14] The spectral separation of the LE and ICT contributions to the total fluorescence spectra was carried out as described previously (see Experimental Section).[14]

It is seen from Figure 11 that the relative contribution of the ICT emission becomes gradually larger with increasing delay time from 3 to 90 ps, with a simultaneous decrease of the LE fluorescence. At time zero, the presence of an ICT emission

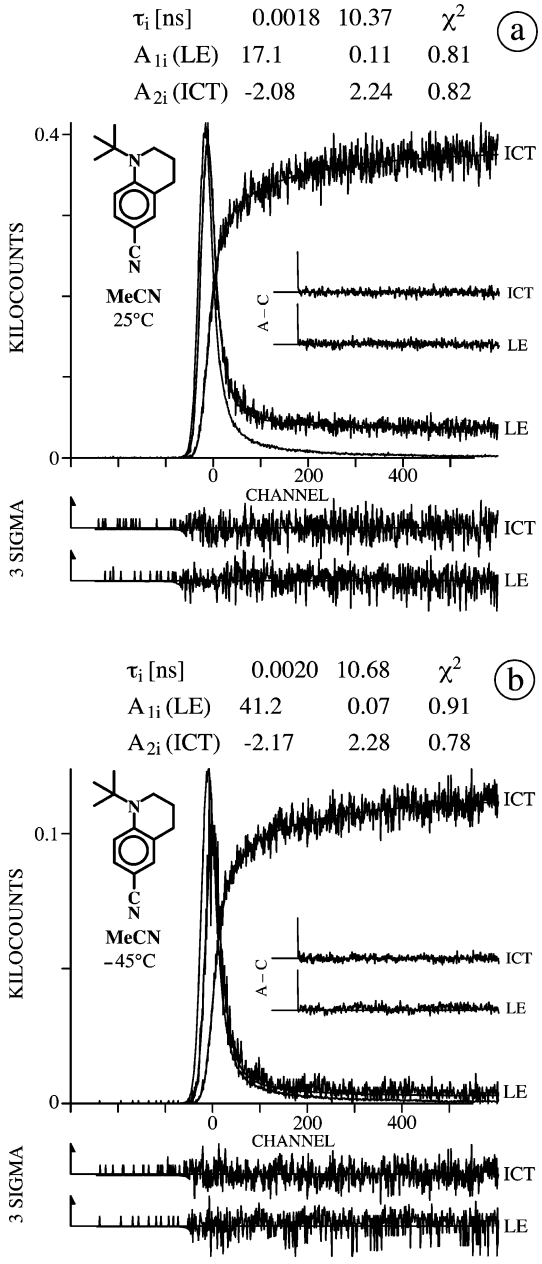

Figure 9. Double exponential LE (340 nm) and ICT (440 nm) fluorescence decays of 1-*tert*-butyl-6-cyano-1,2,3,4-tetrahydroquinoline (NTC6) in acetonitrile (MeCN) at (a) +25 °C and (b) −45 °C. The decay times are τ_2 and τ_1 with the corresponding amplitudes A_{1i}(LE) and A_{2i}(ICT), see eqs 3−5, are given in the figure. The shortest decay time is listed first. The time τ_1 (kept fixed in the global analysis) was determined from the same decays with 10.38 ps/channel. Excitation wavelength λ_{exc}: 276 nm. Time resolution: 0.5 ps/channel with a time window of 600 channels. See the caption of Figure 8.

cannot be detected, as the overall spectrum is indistinguishable from that of LE. It hence follows, similar to what was observed with DMABN in MeCN,[14] that the ICT state of NTC6 in *n*-hexane is formed from the initially excited relaxed LE state and not by direct excitation from S_0 or from the higher excited unrelaxed S_2 state.[10,11,30,32] This conclusion is also reached from the observation that the sum of the amplitudes $A_{21} + A_{22}$ (eq 4) of the ICT fluorescence decays is equal to zero,[2,14,15] as discussed above (Figure 8b).

Time Development of the LE and ICT Band Integrals of NTC6 in *n*-Hexane at −95 °C. The time development of the band integrals BI(LE) and BI(ICT) over the separated LE and ICT fluorescence bands of NTC6 in *n*-hexane at −95 °C (see

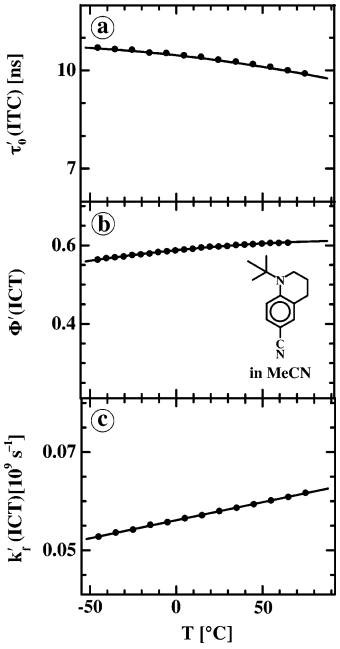

Figure 10. Temperature dependence of (a) the fluorescence decay time τ_0'(ICT) equal to τ_1 (see text), (b) the ICT fluorescence quantum yield Φ'(ICT), and (c) the radiative rate constant k_f'(ICT) for 1-*tert*-butyl-6-cyano-1,2,3,4-tetrahydroquinoline (NTC6) in acetonitrile (MeCN).

Figure 11) is shown in Figure 12. From a global analysis of both integrals, the times $\tau_2 = 19$ ps and $\tau_1 = 4150$ ps, with an amplitude ratio $A = 0.92$ (eqs 3−5), are derived. These decay times are in good agreement with those (20 and 3990 ps) obtained from a global analysis of the LE and ICT fluorescence decays; see Figure 8b. The possibility to fit BI(LE) and BI(ICT) with the same times τ_2 and τ_1 underlines the fact that NTC6 in *n*-hexane at −95 °C undergoes a reversible reaction with two excited states LE and ICT (Scheme 1). The observation that BI(ICT) grows in from zero, i.e., the amplitude ratio $A_{22}/A_{21} = -1.0$ (eq 4), supports our earlier conclusion (see above) that the ICT state is not present at time zero but is formed from the relaxed LE state.[2,3,14,15]

From the decay times (τ_1, τ_2) and the amplitude ratio A (eqs 6 and 7), the rate constants k_a and k_d and also the lifetime τ_0'(ICT) (see Scheme 1) can be determined in the usual manner.[2,14,15] The LE fluorescence decay time of NIC6 at each temperature (no ICT; see above)[3] is adopted here for τ_0(LE). The LE and ICT radiative rate constants can be calculated from k_a, k_d, τ_0(LE), and τ_0'(ICT), together with Φ(LE) for k_f(LE) (see eq 10) and with Φ'(ICT) for k_f'(ICT); see eq 11. The data so obtained are listed in Table 4.

$$k_f(\mathrm{LE}) = \Phi(\mathrm{LE})\{1/\tau_0(\mathrm{LE}) + 1/\tau_0'(\mathrm{ICT})(k_a/(k_d + 1/\tau_0'(\mathrm{ICT}))\} \quad (10)$$

$$k'_f(\mathrm{ICT}) = \Phi'(\mathrm{ICT})\{1/\tau_0'(\mathrm{ICT}) + 1/\tau_0(\mathrm{LE})[(k_d + 1/\tau_0'(\mathrm{ICT}))/k_a]\} \quad (11)$$

NIC6: Transient Absorption Spectra in *n*-Hexane and Acetonitrile. ***n-Hexane.*** The transient absorption spectrum of NIC6 in *n*-hexane at 290 nm excitation is shown in Figure 13a for pump−probe delay times from 0.4 to 120 ps. Similar spectra were measured at $\lambda_{exc} = 266$ nm; see the spectra at 30 ps delay time in Figure 13b. The excited-state absorption (ESA) spectrum, obtained after correction for stimulated emission (SE) is depicted in Figure 13 c.

The ESA spectrum shows strong similarities with the LE(ESA) spectrum of DMABN in *n*-hexane,[14] with maxima at 460 and 750 nm (Table 5) as compared with 445 and 745 nm

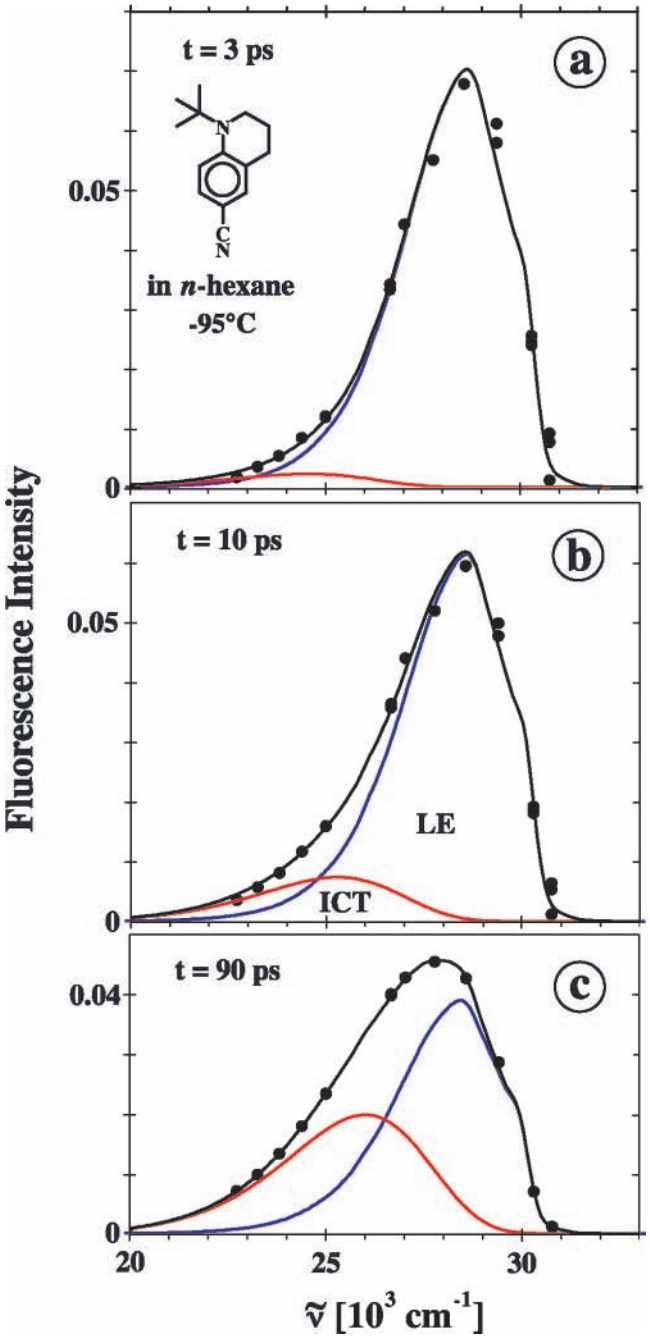

Figure 11. Time-resolved fluorescence spectra of NTC6 in *n*-hexane at −95 °C, at (a) 3 ps, (b) 10 ps, and (c) 90 ps after excitation. The black dots indicate the 17 fluorescence decays from which the total fluorescence spectrum is constructed. See the text for the spectral separation procedure used to obtain the LE (blue) and ICT (red) emission bands. The ICT fluorescence grows from zero, from the primarily excited LE state.

for DMABN. It is seen that the strongest absorption band of NIC6 will have a maximum below 330 nm, outside our present spectral range, in a direction toward the strongest ESA absorption maxima of DMABN at 320 and 300 nm.

MeCN. The transient absorption and ESA spectra of NIC6 in MeCN (Figure 14a,), with pump−probe delay times from 0.1 to 5.0 ps, are similar to those in *n*-hexane (Figure 13). The ESA spectrum in this solvent has absorption maxima at 730 and 450 (Table 5), with the strongest maximum (below 350 nm) now becoming clearly visible. This spectrum should be compared with the ESA spectrum of DMABN in MeCN at

TABLE 4: Data (Scheme 1 and Eqs 3−11) for NTC6 in *n*-Hexane at +25 and −95 °C

T [°C]	τ_2 [ps]	τ_1 [ns]	A	τ_0(LE) [ns]	k_a [10^9 s^{-1}]	k_d [10^9 s^{-1}]	τ'_0(ICT) [ns]	k_f(LE)[a] [10^7 s^{-1}]	$k_{f'}$(ICT)[b] [10^7 s^{-1}]
25[c]	2.1	2.44	0.43	3.0	143	333	1.7	9.3	7.6
25[d]	2.23	2.44	0.39	3.0	126	322	1.7	8.9	8.0
−95[e]	20	3.99	1.08	3.06	26	24	5.6	11	8.2
−95[f]	19	4.15	0.92	3.06	25	27	6.8	10	7.6

[a] Determined by employing eq 10 and Φ(LE) = 0.159 at 25 °C and 0.228 at −95 °C (Table 1). [b] Determined by employing eq 11 and Φ'(ICT) = 0.056 at +25 °C and 0.153 at −95 °C (Table 1). [c] Data from the global analysis of the LE and ICT picosecond fluorescence decays in Figure 8a. The decay time τ_1 comes from measurements at a larger time scale (10.4 ps/channel). [d] Data from a global analysis of the decays in Figure 8a with fixed values for τ_2 and τ_1. The decay time τ_2 is taken from the decay of the femtosecond LE excited-state absorption band in Figure 15c. [e] Data from the global analysis in Figure 8b. The decay time τ_1 comes from measurements at a larger time scale (10.4 ps/channel). [f] Data from the simultaneous analysis of the time development of the LE and ICT band integrals in Figure 12.

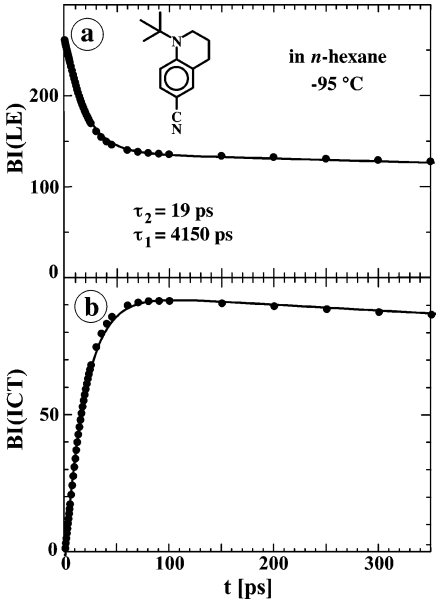

Figure 12. Time development of the band integrals (a) BI(LE) and (b) BI(ICT) over the entire separated LE and ICT fluorescence bands of NTC6 in *n*-hexane at −95 °C (Figure 11). The decay times τ_1 and τ_2, obtained from a global analysis of both integrals, compare favorably with the times (20 and 3990 ps) from the global analysis of the LE and ICT fluorescence decays in Figure 8b. The amplitude ratio A = 0.92 (eq 5) for BI(LE) is close to that from the fluorescence decays (1.08); see text. BI(ICT) is seen to grow in from zero, which means that the ICT state is not present at time zero. This conclusion is supported by the amplitude ratio A_{22}/A_{21} = −1.0 (eq 4) for BI(ICT); see text.

a delay time of 0.2 ps (mainly LE),[14] with maxima at 710, 440, 355, and 320 nm.

The absence of a decay and growing-in in the transient absorption spectra of NIC6 in *n*-hexane and MeCN (Figures 13 and 14), with a time resolution down to 100 fs, again (see above) shows that an ICT state is not formed with this molecule. This observation is in contradiction with the interpretation of gas-phase experiments with NMC6 in the literature, from which it is concluded that an ICT state is populated by passing through an S_2/ICT conical intersection and from there reaches the LE state of lower energy.[32] In the *n*-hexane spectrum, a solvent cooling[14,33] effect is visible (see arrows in Figure 13a), whereas in MeCN a solvation process manifests itself between 0.1 and 1 ps after excitation, with no further evolution after 5 ps (Figure 14a,b). A comparison between the spectra of NIC6 in *n*-hexane and MeCN at 30 ps delay time with an λ_{exc} of 290 and 266 nm (Figures 13b and 14c), shows that these transient absorption spectra do not depend on excitation wavelength. A similar independence was observed for DMABN in MeCN.[14]

NTC6: Transient Absorption Spectra in *n*-Hexane and Acetonitrile. *n*-Hexane. The transient and ESA spectra of NTC6 in *n*-hexane for the spectral range 334−1072 nm (λ_{exc} = 290 nm) are presented in Figure 15a,b for pump−probe delay times between 0.2 and 32 ps (six spectra). For the band with a maximum around 800 nm, a decay of the differential absorbance is observed, whereas around 360 nm a spectral growing-in occurs; see the upward arrow below 400 nm in Figure 15a,b. The decay of the band integral BI(600,970) for the ESA

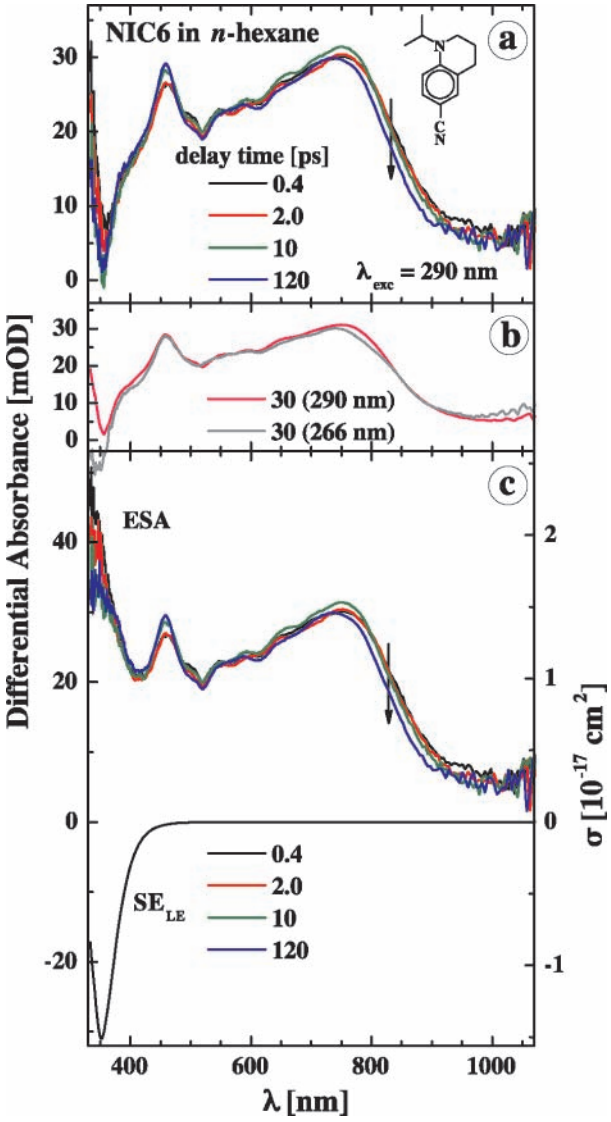

Figure 13. NIC6 in *n*-hexane. (a) Transient absorption spectra (334−1072 nm) with excitation wavelength (λ_{exc}) at 290 nm, for pump−probe delay times between 0.4 and 120 ps. (b) Transient absorption spectra at 30 ps delay time with λ_{exc} at 290 and 266 nm. (c) Excited-state absorption (ESA) spectra after the subtraction of the stimulated emission (SE), at delay times between 0.4 and 120 ps. The SE spectrum is also shown. The cross section σ is given on the right axis. mOD is optical density/1000.

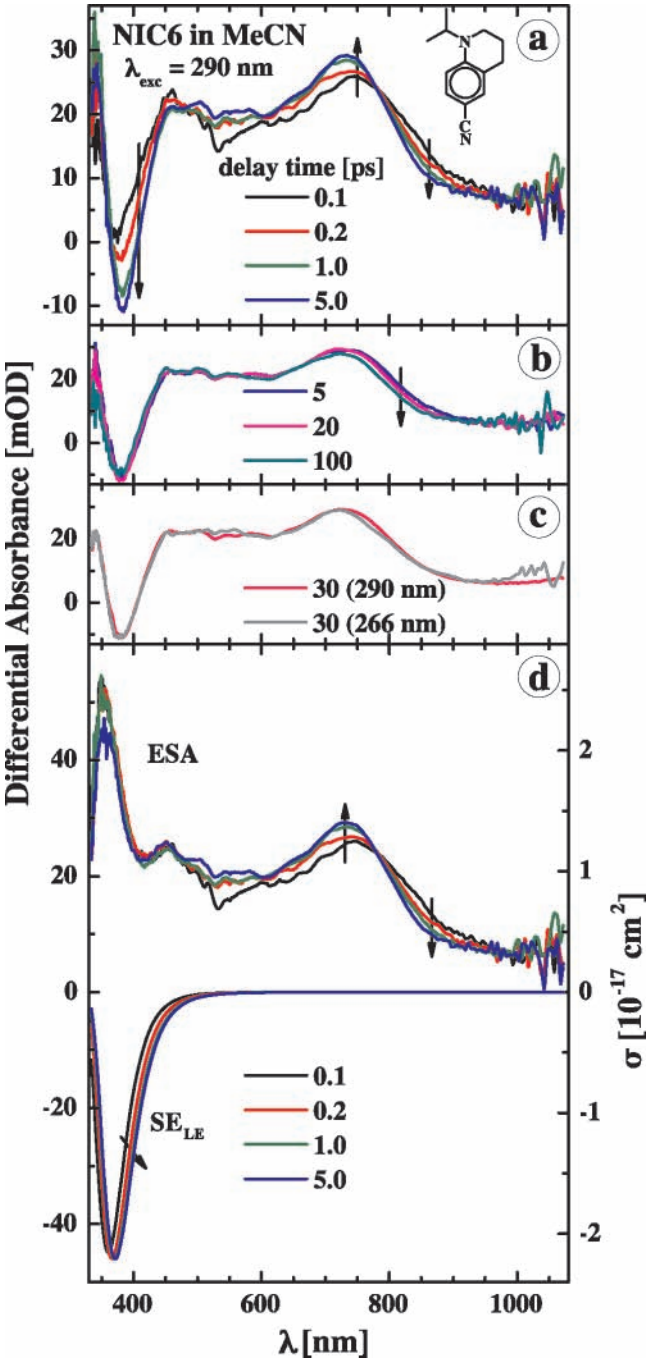

Figure 14. NIC6 in acetonitrile (MeCN). (a) Transient absorption spectra (334−1072 nm) with excitation wavelength (λ_{exc}) at 290 nm, at pump−probe delay times between 0.1 and 5.0 ps. (b) Transient absorption spectra with excitation wavelength (λ_{exc}) at 290 nm, at delay times between 5 and 100 ps. (c) Transient absorption at 30 ps delay time with λ_{exc} at 290 and 266 nm. (d) Excited-state absorption (ESA) spectra after the subtraction of the stimulated emission (SE), at delay times between 0.1 and 5.0 ps. The SE spectra are also shown. The cross section σ is given on the right axis. mOD is optical density/1000.

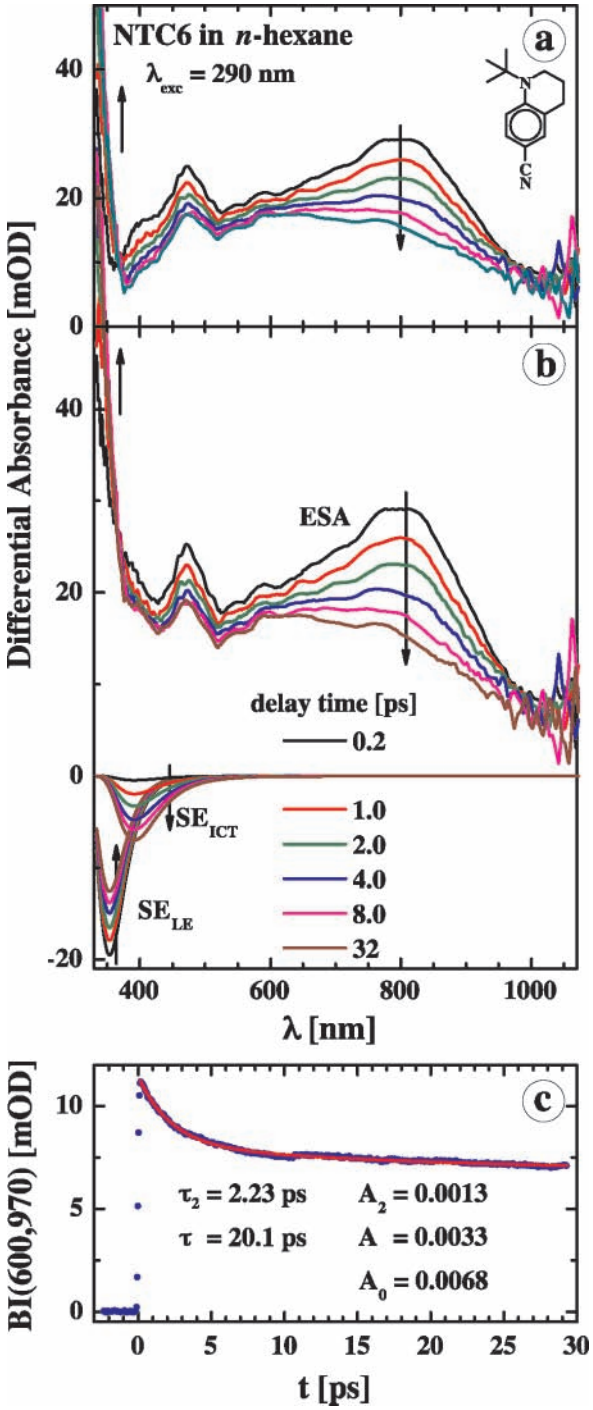

Figure 15. NTC6 in *n*-hexane at 290 nm excitation. (a) Transient absorption spectra (334−1072 nm) and (b) excited-state absorption (ESA) spectra after the subtraction of the stimulated emission (SE), at pump−probe delay times between 0.2 and 32 ps. The LE and ICT SE spectra are also shown. In (a) and (b), the downward arrow (800 nm) indicates the decay of the LE absorption, whereas the upward arrow (below 400 nm) shows the rise of the ICT absorption. (c) Double exponential decay curve of the band integral BI(600,970) between 600 and 970 nm in the ESA spectrum, having decay times τ_2 and τ_1 of 2.23 and 20.1 ps, amplitudes A_2 and A_1 and an offset A_0. mOD is optical density/1000.

spectrum between 600 and 970 nm (Figure 15c), can be fitted with as a double exponential with two decay times of 2.23 and 20.1 ps. The shortest time $\tau_2 = 2.23$ ps obtained from the femtosecond ESA spectrum is to be compared with the decay time $\tau_2 = 2.1$ ps from the picosecond LE and ICT decays of NTC6 in *n*-hexane at 25 °C shown in Figure 8a. This, perhaps surprisingly, good agreement is a verification of the accuracy of the picosecond SPC decays down to 2 ps.

The ESA spectrum of NTC6 in *n*-hexane at the shortest delay time (200 fs) in Figure 15b, closely resembles that of the LE state of NIC6 in this solvent (Figure 13c), with peaks at 470 and 800 nm as compared with 460 and 750 nm for NIC6 (Table 5). In the spectrum of NTC6 there is an onset to a larger peak

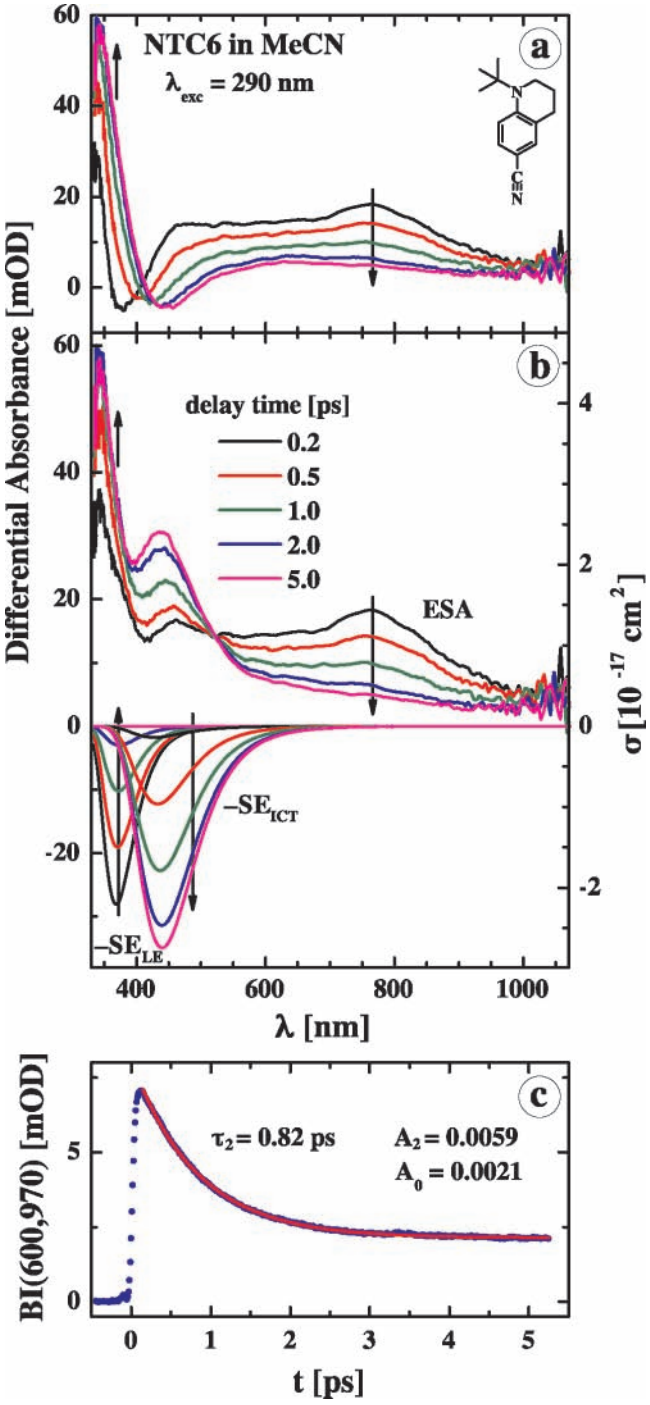

Figure 16. NTC6 in acetonitrile (MeCN) at 290 nm excitation. (a) Transient absorption spectra (334−1072 nm) and (b) excited-state absorption (ESA) spectra after the subtraction of the stimulated emission (SE), at pump−probe delay times between 0.2 and 5.0 ps. The LE and ICT SE spectra are also shown. In (b), the downward arrow (770 nm) indicates the decay of the LE absorption, whereas the upward arrow (below 400 nm) shows the rise of the ICT absorption. (c) Decay curve of the band integral BI(600,970) between 600 and 970 nm in the ESA spectrum, having a decay time τ of 0.82 ps and an offset A_0. mOD is optical density/1000.

below 330 nm, toward the spectral range for the ICT absorption maximum of DMABN (in MeCN)[14] at 315 nm. The decay of the band of NTC6 at 800 nm therefore represents the decay of the absorption of the LE precursor, whereas the rise below 400 nm is due to the formation of the ICT state.

MeCN at λ_{exc} = 290 nm. The transient and ESA spectra of NTC6 in MeCN for λ_{exc} = 290 nm are shown in Figure 16,

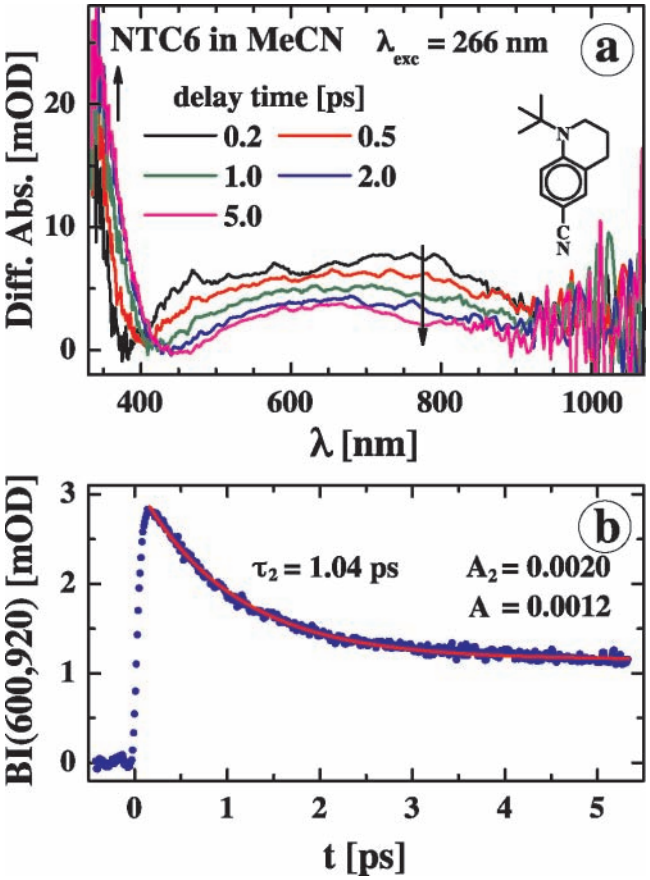

Figure 17. NTC6 in acetonitrile (MeCN) at 266 nm excitation. (a) Transient absorption spectra (334−1072 nm) at pump−probe delay times between 0.2 and 5.0 ps. The downward arrow (770 nm) indicates the decay of the LE absorption, whereas the upward arrow (below 400 nm) shows the rise of the ICT absorption. (b) Decay curve of the band integral BI(600,920) between 600 and 920 nm in the transient absorption spectrum, having a decay time τ of 1.04 ps and an offset A_0. mOD is optical density/1000.

with delay times between 0.2 and 5.0 ps. Similar to what is observed for NTC6 in *n*-hexane (Figure 15), the band having a maximum at 770 nm decays with increasing delay time, whereas a growing-in is observed below 400 nm (upward arrow). The decay of BI(600,970) can be fitted with a single decay time τ of 0.82 ps and an offset A_0; see Figure 16c.

The ESA spectrum at the shortest delay time of 200 fs (Figure 16b) is that of the LE state. This identification of the absorption spectrum, with maxima at 765, 460, and below 334 nm (Table 5), is based on the similarity with the LE(ESA) spectrum of NIC6 in MeCN (Figure 14d), having maxima at 730 and 450 nm. The decay of the LE absorption band is accompanied by a spectral growing-in around 440 nm and below the spectral window at 334 nm (Figure 16b). As already mentioned in the previous section, the main ICT peak of DMABN in MeCN is found at 315 nm and a smaller band occurs at 425 nm. It is therefore concluded that the ICT state of NTC6 in MeCN is formed from the LE precursor, the same conclusion as for *n*-hexane (Figure 15b).

MeCN at λ_{exc} = 266 nm. The decay and rise pattern of the transient absorption spectra of NTC6 in MeCN for 266 nm excitation (Figure 17a) is similar to that found for the spectra with λ_{exc} = 290 nm in Figure 16. The somewhat lower quality of the spectra in Figure 17 as compared with Figure 16, is due to the fact that the molar absorption coefficient (Table 2) of NTC6 in MeCN is much smaller at 266 (1370 M^{-1} cm^{-1}) than at 290 nm (13520 M^{-1} cm^{-1}).

TABLE 5: Excited-State Absorption (ESA) Maxima and Decay Times τ_2 for NTC6 and NIC6 in *n*-Hexane and Acetonitrile (MeCN) (Figures 13−16)

	ESA maxima [nm]		decay times τ_2 [ps][a]	
	n-hexane	MeCN	*n*-hexane	MeCN
NTC6	470, 800	765, 460, below 334	2.23	0.82[b]
NIC6	460, 750	730, 450, below 350		
DMABN (LE)[c]	300, 320, 445, 470, 745	320, 355, 440, 710		
DMABN (ICT)[c]		315, 425, (490), 970		4.07

[a] Excitation at 290 nm. [b] 1.04 ps at 266 nm excitation (Figure 17); see text. [c] Data from ref 14.

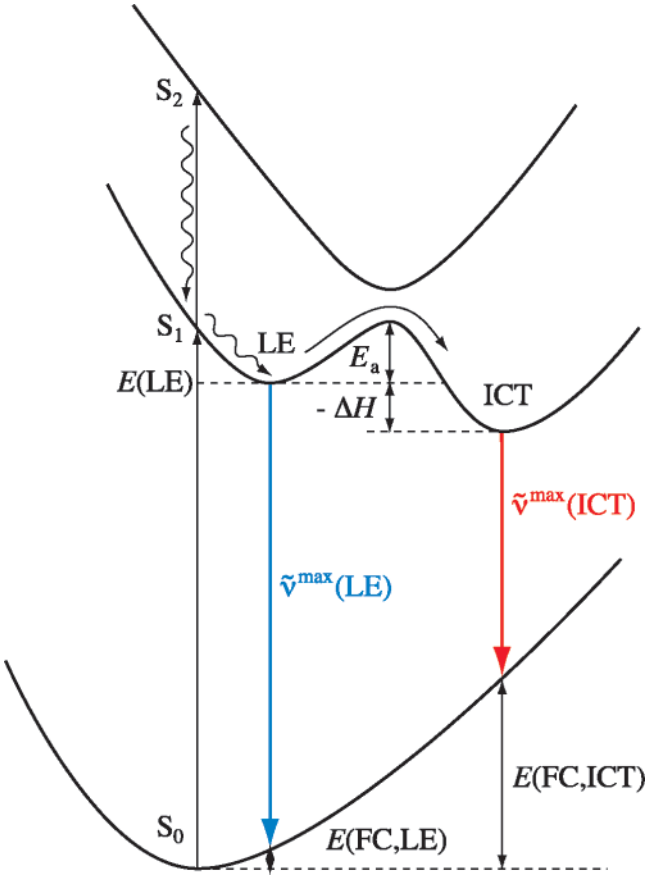

Figure 18. Potential energy surfaces for the ground state S_0 and the excited states S_1, S_2, LE, and ICT. When excited to the S_2 state (with an energy gap $\Delta E(S_1,S_2)$ above S_1), the system relaxes by internal conversion to the equilibrated LE state, having an energy E(LE) above S_0. The ICT reaction proceeds from the LE to the ICT state, with a reaction barrier E_a and an enthalpy difference ΔH. Fluorescence from the LE and ICT states, with emission maxima $\tilde{\nu}^{max}$(LE) and $\tilde{\nu}^{max}$(ICT), reaches the corresponding Franck−Condon states E(FC,LE) and E(FC,ICT).

The band integral BI(600,920) for the ESA spectrum can be fitted as a single exponential (Figure 17b) with a decay time of 1.04 ps, slightly longer than the time of 0.82 ps for $\lambda_{exc} = 290$ nm in Figure 16c.

Intramolecular Charge Transfer with NTC6 in *n*-Hexane and MeCN. It is seen from the ESA spectra (Figures 15−17) that NTC6 undergoes a fast ICT reaction (2.2 ps) in *n*-hexane, whereas such a reaction does not take place with DMABN in this solvent.[14] With NTC6 in MeCN, a subpicosecond ICT reaction (0.82 ps) is observed, as compared with 4 ps reaction for DMABN.[14] The observation that the shortest decay time τ_2 of NTC6 in MeCN ($\epsilon^{25} = 36.7$) is considerably shorter than in *n*-hexane ($\epsilon^{25} = 1.88$) reflects the generally observed[7,14,15] increase in the rate constant k_a for the LE → ICT reaction of aminobenzonitriles (Scheme 1) when the solvent polarity becomes larger. The LE(ESA) spectrum of NTC6 in *n*-hexane as well as in MeCN (at 200 fs after excitation) is comparable to that of NIC6 in both solvents, indicating that these LE states have a similar molecular structure, in contrast to the expectation based on recent computations.[11]

ICT Mechanism for NTC6. The decay of the LE absorption and the corresponding growing-in for the ICT state in the ESA spectra of NTC6 in *n*-hexane as well as MeCN at room temperature (Figures 15−17) makes clear that the ICT state originates from the LE precursor (Figure 18). The observation that for NTC6 in MeCN the transient spectra and their time development is the same for 266 and 290 nm excitation is in line with this interpretation. The conclusion that there is no ICT fluorescence at the moment of excitation was already made from the global analysis of the ICT SPC decay curve (Figure 8b) and also from the time-resolved fluorescence spectra (Figure 11).

Our conclusion that the ICT state is not present at time zero, is in contradiction to the results of calculations[10,11] and the interpretation of gas-phase experiments with NMC6 and DMABN,[32,34] from which it is concluded that the ICT as well as the LE state are formed via an S_2/ICT conical intersection. Within this mechanism, ICT and LE can appear simultaneously, i.e., LE is not the precursor of ICT.

Conclusions

With the rigidized molecule NTC6, dual fluorescence (LE + ICT) is observed in the nonpolar solvent *n*-hexane as well as in the polar MeCN, whereas only LE emission is found for its *N*-isopropyl derivative NIC6, even in MeCN at −45 °C. The absence of ICT in the case of NIC6 is attributed to its larger energy gap $\Delta E(S_1,S_2)$ as compared with NTC6 (Figure 18). From the temperature dependence of the quantum yield ratio Φ'(ICT)/Φ(LE) for NTC6 in *n*-hexane an enthalpy difference ΔH of −2.4 kJ/mol is calculated for the LE → ICT reaction.

By measuring the molar absorption coefficients ϵ^{max} of NTC6 and NIC6, together with a number of their derivatives, an amino twist angle θ between 21 and 23° is determined for the ground state of NTC6 in *n*-hexane. It is found that the ϵ^{max} of NTC6 becomes larger when going from *n*-hexane to MeCN, from which it is concluded that the amino group of NTC6 becomes less twisted with increasing solvent polarity.

With NIC6 in *n*-hexane from +65 to −95 °C as well as in MeCN from +75 to −45 °C, single-exponential picosecond SPC fluorescence decays are observed, supporting the conclusion based on the photostationary LE emission spectra that ICT does not occur with this molecule. For NTC6 in *n*-hexane and MeCN, the LE and ICT fluorescence decays are double exponential. Whereas the shortest decay time τ_2 of 2.1 ps for NTC6 in *n*-hexane at +25 °C appears to be at the limit of the SPC time resolution, τ_2 increases to 20 ps at −95 °C in this solvent, making the measurement of time-resolved emission spectra possible at this temperature. From the time development of these spectra it is seen that the ICT state grows in from zero, indicating that the LE state is the precursor in the ICT reaction of NTC6.

By analyzing the LE and ICT band integrals derived from the time-resolved spectra, the following results are obtained: $\tau_2 =$ 19 ps and $\tau_1 = 4.15$ ns with an amplitude ratio of 0.92. The forward and backward ICT rate constants (Scheme 1), $k_a = 2.5 \times 10^{10}$ s^{-1} and $k_d = 2.7 \times 10^{10}$ s^{-1}, calculated from these data show that the ICT reaction is still fast for NTC6 at −95 °C.

The absence of a decay and growing-in in the transient absorption spectra of NIC6 in *n*-hexane and MeCN, with a time resolution down to 100 fs, again shows that an ICT state is not formed with this molecule, in contradiction of the interpretation of gas-phase experiments with NMC6 in the literature, from which it is concluded that an ICT state is populated by passing through an S_2/ICT conical intersection and then reaches the LE state of lower energy. With NTC6, the transient spectra consist of contributions from the LE and ICT state. The decay of the LE absorption and the corresponding growing-in for the ICT state make clear that LE is the precursor in the ICT reaction, i.e., that the ICT and LE states are not formed simultaneously from an S_2/ICT conical intersection. This conclusion supports the observation mentioned above that in the picosecond time-resolved fluorescence spectra ICT emission is absent at the moment of excitation. From the decay of the band integrals of the ESA spectra, with shortest decay times τ_2 of 2.2 ps in *n*-hexane and 0.82 ps MeCN, it appears that ICT with NTC6 becomes faster with increasing solvent polarity. With DMABN, the ICT reaction in MeCN is considerably slower ($\tau_2 = 4.0$ ps at 25 °C) than for NTC6 and ICT does not take place in *n*-hexane. For NTC6 in MeCN, the ESA spectra and their time development are the same for $\lambda_{exc} = 290$ and 266 nm. This independence of excitation wavelength is in line with our conclusion that LE is the ICT precursor.

The transient absorption spectrum of NTC6 in *n*-hexane and MeCN at 200 fs after excitation is similar to the LE(ESA) spectra of NIC6 and DMABN, showing that LE is the initially excited state for NTC6. The spectral similarity also indicates that the LE states of NTC6, NIC6, and DMABN have a comparable molecular structure. The same conclusion is made for the structure of the ICT states of NTC6 and DMABN, as the ICT(ESA) spectrum of NTC6 in *n*-hexane and MeCN resembles that of DMABN in MeCN.

Acknowledgment. We thank Dr Attila Demeter (Chemical Research Center, Budapest) for measuring the intersystem crossing yield of NTC6. Many thanks are due to Mr. Jürgen Bienert for carrying out HPLC purifications and to Mr. Wilfried Bosch and Mr. Helmut Lesche for technical support.

Supporting Information Available: Figure showing absorption and fluorescnce cross section spectra of NTC6 in *n*-hexane and acetonitrile. This material is available free of charge via the Internet at http://pubs.acs.org.

References and Notes

(1) Visser, R. J.; Varma, C. A. G. O. *J. Chem. Soc., Faraday Trans. 2* **1980**, *76*, 453.

(2) Leinhos, U.; Kühnle, W.; Zachariasse, K. A. *J. Phys. Chem.* **1991**, *95*, 2013.

(3) Zachariasse, K. A.; Druzhinin, S. I.; Bosch, W.; Machinek, R. *J. Am. Chem. Soc.* **2004**, *126*, 1705.

(4) Rotkiewicz, K.; Grabowski, Z. R.; Krówczyński, A.; Kühnle, W. *J. Luminescence* **1976**, *12/13*, 877.

(5) Grabowski, Z. R.; Rotkiewicz, K.; Rubaszewska, W.; Kirkor-Kaminska, E. *Acta Phys. Polon.* **1978**, *54A*, 767.

(6) Günter, W.; Rettig, W. *J. Phys. Chem.* **1984**, *88*, 2729.

(7) Grabowski, Z. R.; Rotkiewicz, K.; Rettig, W. *Chem. Rev.* **2003**, *103*, 3899.

(8) Yoshihara, T.; Druzhinin, S. I.; Zachariasse, K. A. *J. Am. Chem. Soc.* **2004**, *126*, 8535.

(9) Amatatsu, Y. *J. Phys. Chem. A* **2005**, *109*, 7225.

(10) Gómez, I.; Mercier, Y.; Reguero, M. *J. Phys. Chem. A* **2006**, *110*, 11455.

(11) Hättig, C.; Hellweg, A.; Köhn, A. *J. Am. Chem. Soc.* **2006**, *128*, 15672.

(12) Zachariasse, K. A.; Grobys, M.; von der Haar, Th.; Hebecker, A.; Il'ichev, Yu. V.; Morawski, O.; Rückert, I.; Kühnle, W. *J. Photochem. Photobiol. A: Chem.* **1997**, *105*, 373.

(13) Braslavsky, S. E. *Pure Appl. Chem.* **2007**, *79*, 293.

(14) Druzhinin, S. I.; Ernsting, N. P.; Kovalenko, S. A.; Lustres, L. P.; Senyushkina, T. A.; Zachariasse, K. A. *J. Phys. Chem. A* **2006**, *110*, 2955.

(15) Yoshihara, T.; Druzhinin. S. I.; Demeter, A.; Kocher, N.; Stalke, D.; Zachariasse, K. A. *J. Phys. Chem. A* **2005**, *109*, 1497.

(16) Galievsky, V. A.; Druzhinin, S. I.; Demeter, A.; Jiang, Y.-B.; Kovalenko, S. A.; Lustres, L. P.; Venugopal, K.; Ernsting, N. P.; Allonas, X.; Noltemeyer, M.; Machinek, R.; Zachariasse, K. A. *Chem. Phys. Chem.* **2005**, *6*, 2307.

(17) Kovalenko, S. A.; Dobryakov, A. L.; Ruthmann, J.; Ernsting, N. P. *Phys. Rev. A* **1999**, *59*, 2369.

(18) Ernsting, N. P.; Kovalenko, S. A.; Senyushkina, T. A.; Saam, J.; Farztdinov, V. *J. Phys. Chem. A* **2001**, *105*, 3443.

(19) Yoshihara, T.; Galievsky, V. A.; Druzhinin. S. I.; Saha, S.; Zachariasse, K. A. *Photochem. Photobiol. Sci.* **2003**, *2*, 342.

(20) In ref 3, the ICT fluorescence spectrum was obtained by subtracting the LE emission spectrum of NIC6 from the total fluorescence spectrum of NTC6, giving somewhat different results. This difference in procedure does practically not affect the slope of the plot for $\ln(\Phi'(\mathrm{ICT})/\Phi(\mathrm{LE}))$ *versus* the reciprocal absolute temperature (see Figure 4).

(21) Suzuki, K.; Demeter, A.; Kühnle, W.; Tauer, E.; Zachariasse, K. A. *Phys. Chem. Chem. Phys.* **2000**, *2*, 981.

(22) The data for ϵ^{max} of NTC6, NIC6, NEC6, and NMC6 in *n*-hexane listed in Table 2 are somewhat different from those reported in Table 1 of our previous publication ref 3. The reason for this discrepancy is not clear. Our present data have been obtained from repeated measurements with carefully purified compounds (fresh HPLC) and a comparison with well-established data such as those of DMABN (Table 2).

(23) Burgers, J.; Hoefnagel, M. A.; Verkade, P. E.; Visser, H.; Wepster, B. M. *Recl. Trav. Chim. Pays-Bas* **1958**, *77*, 491.

(24) Rückert, I.; Hebecker, A.; Parusel, A. B. J.; Zachariasse, K. A. *Z. Phys. Chem.* **2000**, *214*, 1597.

(25) Druzhinin, S. I.; Noltemeyer, M.; Zachariasse, K. A. Paper in preparation.

(26) Landolt-Börnstein, *Numerical Data and Functional Relationships in Science and Technology*, *New Series*; Madelung, O., Ed.; Springer: Berlin, 1991; Group IV, Vol. 6.

(27) For systems with small $-\Delta H$, the thermal ICT → LE back reaction (k_d, Scheme 1) often becomes large relative to $1/\tau'_0$(ICT) already at room temperature. This high-temperature-limit (HTL) condition leads to small values for $\Phi'(\mathrm{ICT})/\Phi(\mathrm{LE})$; see eqs 1 and 2 (refs 2 and 14). The maximum value for $\Phi'(\mathrm{ICT})/\Phi(\mathrm{LE})$ is reached when $k_d = 1/\tau'_0(\mathrm{ICT})$, which then obviously can be brought about by lowering the temperature.

(28) Druzhinin, S. I.; Demeter, A.; Galievsky, V. A.; Yoshihara, T.; Zachariasse, K. A. *J. Phys. Chem. A* **2003**, *107*, 8075.

(29) Landolt-Börnstein. *Numerical Data and Functional Relationships in Science and Technology*, *New Series*; Lechner, M. D., Ed.; Springer, Berlin, 1996; Group III, Vol. 38B.

(30) Gómez, I.; Reguero, M.; Boggio-Pasqua, M.; Robb, M. A. *J. Am. Chem. Soc.* **2005**, *127*, 7119.

(31) Birks, J. B. *Photophysics of Aromatic Molecules*; Wiley: London, 1970.

(32) Fuss, W.; Schmid, W. E.; Pushpa, K. K.; Trushin, S. A.; Yatsuhashi, T. *Phys. Chem. Chem. Phys.* **2007**, *9*, 1151.

(33) Schwarzer, D.; Troe, J.; Zerezke, M. *J. Chem. Phys.* **1997**, *107*, 8380.

(34) Fuss, W.; Rettig, W.; Schmid, W. E.; Trushin, S. A.; Yatsuhashi, T. *Faraday Discuss.* **2004**, *127*, 23.